

---

Retrospective Theses and Dissertations

---

1987

## Motion and Intrusion Detection Using a Pyroelectric Detector

Randy R. Fields  
*University of Central Florida*

 Part of the [Engineering Commons](#)

Find similar works at: <https://stars.library.ucf.edu/rtd>

University of Central Florida Libraries <http://library.ucf.edu>

This Doctoral Dissertation (Open Access) is brought to you for free and open access by STARS. It has been accepted for inclusion in Retrospective Theses and Dissertations by an authorized administrator of STARS. For more information, please contact [STARS@ucf.edu](mailto:STARS@ucf.edu).

---

### STARS Citation

Fields, Randy R., "Motion and Intrusion Detection Using a Pyroelectric Detector" (1987). *Retrospective Theses and Dissertations*. 5073.

<https://stars.library.ucf.edu/rtd/5073>

MOTION AND INTRUSION DETECTION USING A PYROELECTRIC  
DETECTOR

BY

RANDY R. FIELDS  
B.S.E., University of Central Florida, 1983

THESIS

Submitted in partial fulfillment of the requirements  
for the degree of Master of Science in Engineering  
in the Graduate Studies Program  
of the College of Engineering  
of the University of Central Florida  
Orlando, Florida

Summer Term  
1987

## ABSTRACT

The purpose of this paper is to describe a device that passively detects the presence of a warm-bodied object in a specified area. The detecting device used is a pyroelectric detector with an integral optical filter. By focusing infrared radiation generated by the object onto the detector, the resulting temperature change is converted to a voltage and then amplified. Modulation of the incoming radiation is accomplished by a rotating disk whose speed of rotation is dynamically controlled by a microprocessor. The resulting detector response is filtered and converted to a DC level. The signal is then passed through an analog-to-digital converter and sampled by the microprocessor.

## TABLE OF CONTENTS

Introduction . . . . .	1
Pyroelectric Detectors . . . . .	3
An Application of the Pyroelectric Effect . . . . .	8
Detector Selection . . . . .	11
Modulator Design . . . . .	12
Amplification . . . . .	15
Band Pass Filter Design . . . . .	21
Absolute Value Circuit . . . . .	28
Signal Processing . . . . .	33
Summary . . . . .	34
Appendix . . . . .	35
References . . . . .	45

## INTRODUCTION

Some 2300 years ago, around 400 B.C., the Greeks observed that when heated in a fire, a tourmaline crystal would first attract and then repel small particles of dust and ash. The particles were inductively attracted to the crystal and upon making contact would accept a charge. The charged particles were then repelled because of the forces of like charges. It was not until 1824 in England that the effect would be studied and named pyroelectricity by D. Brewster[1].

A pyroelectric crystal is a member of the piezoelectric class of crystals that possesses a spontaneous polarization along an axis within its structure. Spontaneous polarization is characterized as the presence of polar atoms in a crystal lattice creating a natural electric moment per unit volume. There are 10 classes of crystal point groups that have this structure. In most cases, the presence of the electric field produced by this polarization is undetectable because of the free flow of charge within the crystal to the surface causing a cancelation of any external electric field. However, a change in

temperature of a pyroelectric crystal will result in a rotation of the internal dipole moment and hence a change in the surface charge present. This uniform dipole rotation is maintained in the crystal below the curie point for the material. When temperature equilibrium is attained the flow of free charge to the crystal surface will again cancel any external electric field produced by the internal polarization. Above the curie point the materials will depole and produce no net polarization[2,3,4].

## PYROELECTRIC DETECTORS

Devices have been constructed based on the pyroelectric effect that can detect very small changes in temperature. These devices, called pyroelectric detectors, usually consist of a thin slab of a pyroelectric crystal placed between two parallel electrodes. The crystalline material comprising the detector element is usually of very low conductivity. Physically the detector has the two electrodes contacting the natural surface charge of the element separated by a highly insulating material, which in effect forms and can be modeled as a parallel plate capacitor. The response of a detector is proportional to the rate of change of temperature. Changes in the device temperature will induce an electrical current in a circuit connected to the detector electrodes. Therefore a model of the detector would require the addition of a voltage source in series with or a current source in parallel with the capacitor. Since the crystal material of the detector has some finite resistance, a simple model for the device would be completed by including a high resistance across the electrodes[6], as shown in Figure 1.

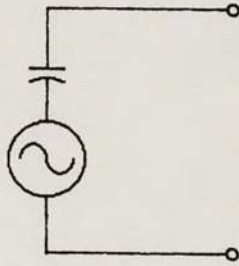


Figure 1. Model for a Pyroelectric Detector

A pyroelectric detector will respond to a change of temperature from any source with a voltage change at the electrodes. This source of temperature change could come from many sources including vibration, conduction, or radiation. The voltage response will be proportional to the rate of temperature change. The response of a pyroelectric device to a change in temperature  $T$  can be expressed mathematically[1] as follows:

$$C^{E_bA} \frac{d \Delta T}{dt} + g_r A \Delta T = \eta [P_0 + P_1 e^{j \omega t}]$$



where:

$C^E$  = volume specific heat

$b$  = thickness of the detector element

$A$  = area of the detector element

$\eta$  = fraction of incident power converted to heat

$g_r$  = radiated loss conductance per unit area

$P_0 + P_1 e^{j \omega t}$  = incoming radiation power modulated at frequency  $\omega$ .

The steady state solution of the equation can be derived as follows:

Dividing each term by  $(C^E b A)$  yields

$$\frac{d \Delta T}{dt} + \frac{g_r}{C^E b} \Delta T = \frac{\eta}{C^E b A} [P_0 + P_1 e^{j \omega t}]$$

This is the standard form of a first-order linear differential equation. An integrating factor for this equation would be:

$$\exp \left[ \int K dt \right] \quad \text{where } K = \frac{g_r}{C^E b}$$

or

$$e^{Kt}$$

Multiplying through by the integrating factor yields

$$e^{Kt} \frac{d \Delta T}{dt} + K e^{Kt} \Delta T = \frac{\eta}{C^E b A} [P_0 + P_1 e^{j \omega t}] e^{Kt}$$

This can now be rewritten as:

$$\frac{d}{dt} e^{K \Delta T} = \frac{\eta}{C^E b A} P_1 e^{(K + j \omega) t}$$

Integrating this equation yields:

$$K \Delta T = \frac{\eta}{C^E b A} P_1 \int e^{(K + j \omega) t}$$

and

$$\Delta T = \frac{\eta}{C^E b A} P_1 \left[ \frac{1}{K + j \omega} \right] e^{j \omega t}$$

Now a change of temperature causes a change in surface charge of

$$Q(\omega, t) = A \Delta P = p A \Delta T(\omega, t)$$

which results in a voltage change of

$$\Delta V(\omega, t) = \frac{Q(\omega, t)}{C_d} = \frac{p}{\kappa \epsilon} b \Delta T(\omega, t)$$

The responsivity of the detector is defined as

$$R_V = \frac{\eta p}{C^E \kappa \epsilon A} \frac{\tau}{(1 + \omega^2 \tau^2)^{1/2}}$$

where  $\tau$  is the device time constant.

The voltage produced by a change in temperature would then be

$$V_{\text{rms}} = R_V P_1$$

## AN APPLICATION OF THE PYROELECTRIC EFFECT

The pyroelectric effect depends only on a change in temperature from any source to generate a detectable signal that can be processed and used in a system. An application of the effect is to use a detector to passively determine the presence of a warm-bodied animal or human in a specified area. The graph shown in Figure 2 shows the relationship between the temperature of an object and the wavelength of maximum energy generated by that object[7]. Also shown is the emitted blackbody radiation in  $W/cm^2$ .

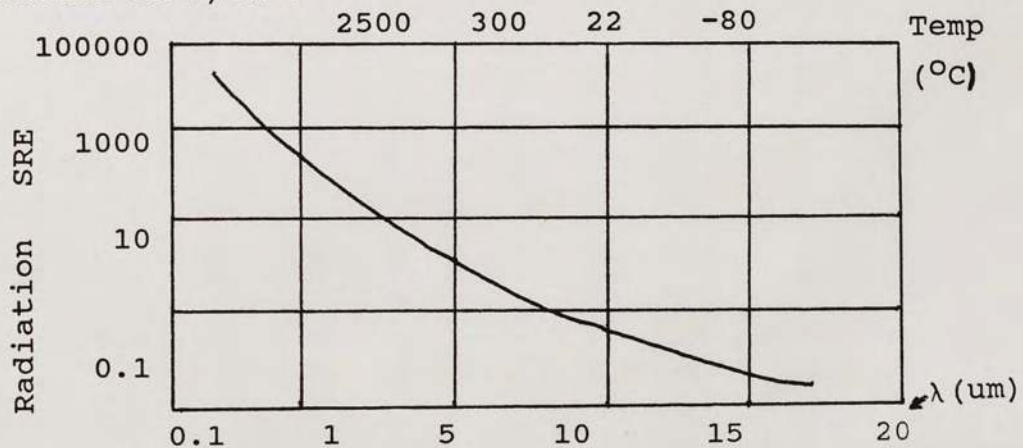


Figure 2. Graph of Temperature vs. Maximum Energy

By focusing this energy onto a detector, a change in temperature will result, causing a voltage response. For a human, the distribution of emitted wavelengths[7]

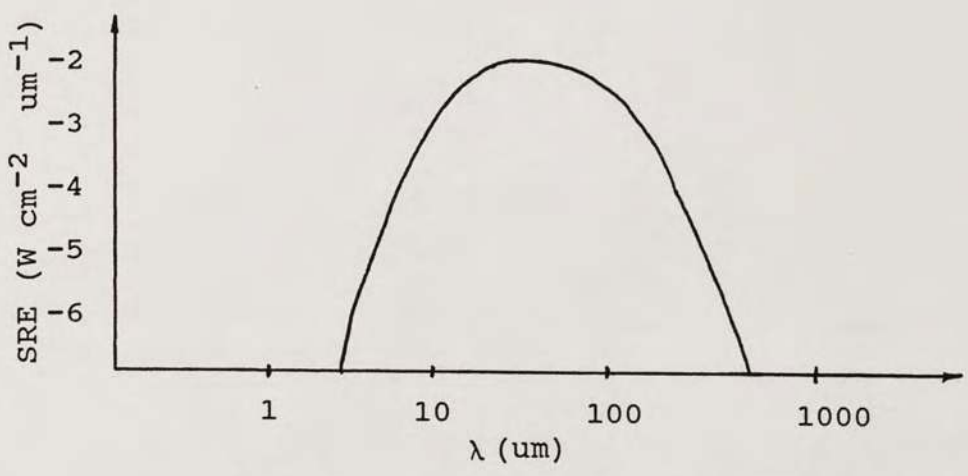


Figure 3. Wavelengths Emitted by Humans

is as shown in Figure 3. Since the spectrum of wavelengths that pertains to the object that is to be detected centers around 10um, an optical filter could be used to minimize the detectors response to other sources of temperature change. Figure 3a shows the transmissive properties of some materials that could be used in this application.

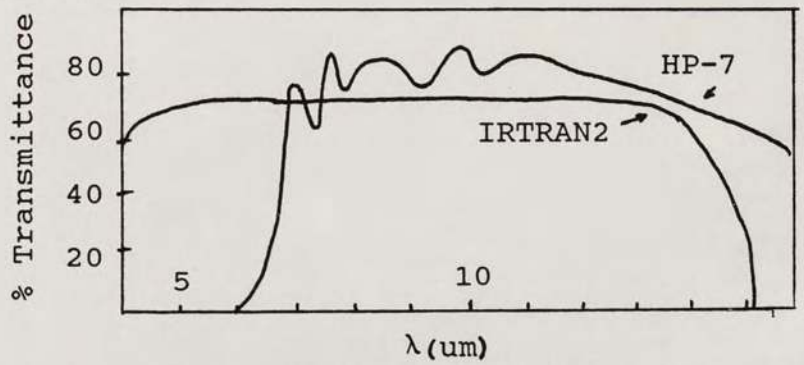


Figure 3a. Transmissive Properties of Some Materials

The amount of infrared energy generated by an intruder is very small so a lens is used to focus the incoming radiation onto the detector. Since the signal

falling on the detector must be constantly changing to generate a voltage across the electrodes of the device, the heat radiated by the intruder will be modulated at the detector to provide a constantly changing signal. A bandpass filter at the modulation frequency will be designed to eliminate the response of the detector to other sources of temperature change. The magnitude of the resulting signal will be converted to a digital signal that can be sampled by a microprocessor and used to respond to the presence of an intruder.

## DETECTOR SELECTION

The selected detector must respond to the wavelengths generated by an intruder as shown in Figure 3. Since the pyroelectric effect depends only on the change of temperature of the detector, almost any pyroelectric device would work in this application. By using an optical filter with the detector, some undesired signals could be prevented from entering the system and generating false responses. Therefore a detector was chosen with a built-in optical filter that would pass primarily the frequencies generated in the range of interest. The Eltec 406 specifications[7] are as shown in Figure 4.

Characteristics		406	Unit	Test Conditions	ELTECdata Reference
Detector Type		Single	—		
Element Size		2.0	mm, DIA	nominal	
Optical Bandwidth		1.5 to 1000	$\mu\text{m}$	Various Windows	101
Responsivity	min	3000	V/W	8 to 14 $\mu\text{m}$ @1Hz	
	typ	3600			
	max	4200			
Noise	typ	10	$\mu\text{V}/\sqrt{\text{Hz}}$	1.0Hz p-p (1 minute)	
	max	20			
NEP	typ	$7.0 \times 10^{-10}$	$\text{W}/\sqrt{\text{Hz}}$	8-14 $\mu\text{m}$ (@ 1Hz, BW 1Hz)	100
	max	$1.7 \times 10^{-9}$			
D*	min	$1.0 \times 10^8$	$\text{cm}\sqrt{\text{Hz}}/\text{W}$	8-14 $\mu\text{m}$ (@ 1Hz, BW 1Hz)	100
	typ	$2.5 \times 10^8$			
Operating Voltage	min	3	V	$V_D$ to Gnd	104 (4.1.c)
	max	15			
Operating Current	min	0.1	$\mu\text{A}$		104 (4.1.c)
	max	40			

Figure 4. Eltec 406 Specifications

## MODULATOR DESIGN

The incoming infrared radiation generated by the intruder is modulated by an opaque rotating disk placed in front of the pyroelectric detector. A small DC motor is directly connected to a shaft on top of which the modulation disk is mounted. The speed of the motor must be dynamically controlled to insure the correct modulation frequency of the incoming radiation. Since the speed of the motor is dependant on the voltage supplied, the microprocessor can provide speed control by changing this voltage. A pulse width modulation scheme was employed where a constant frequency pulse stream generated by the microprocessor was filtered to produce a digitally controllable DC voltage level. This voltage level is determined by the duty cycle of the pulse stream. To monitor its speed of rotation a small disk is mounted perpendicularly to the motor shaft. The small disk has an opening at one point in its circumference. An infrared light emitting diode is placed on one side of the disk while an infrared sensitive phototransistor is mounted across from the LED on the other side of the small disk. As the motor turns the opening in the disk circumference will allow the



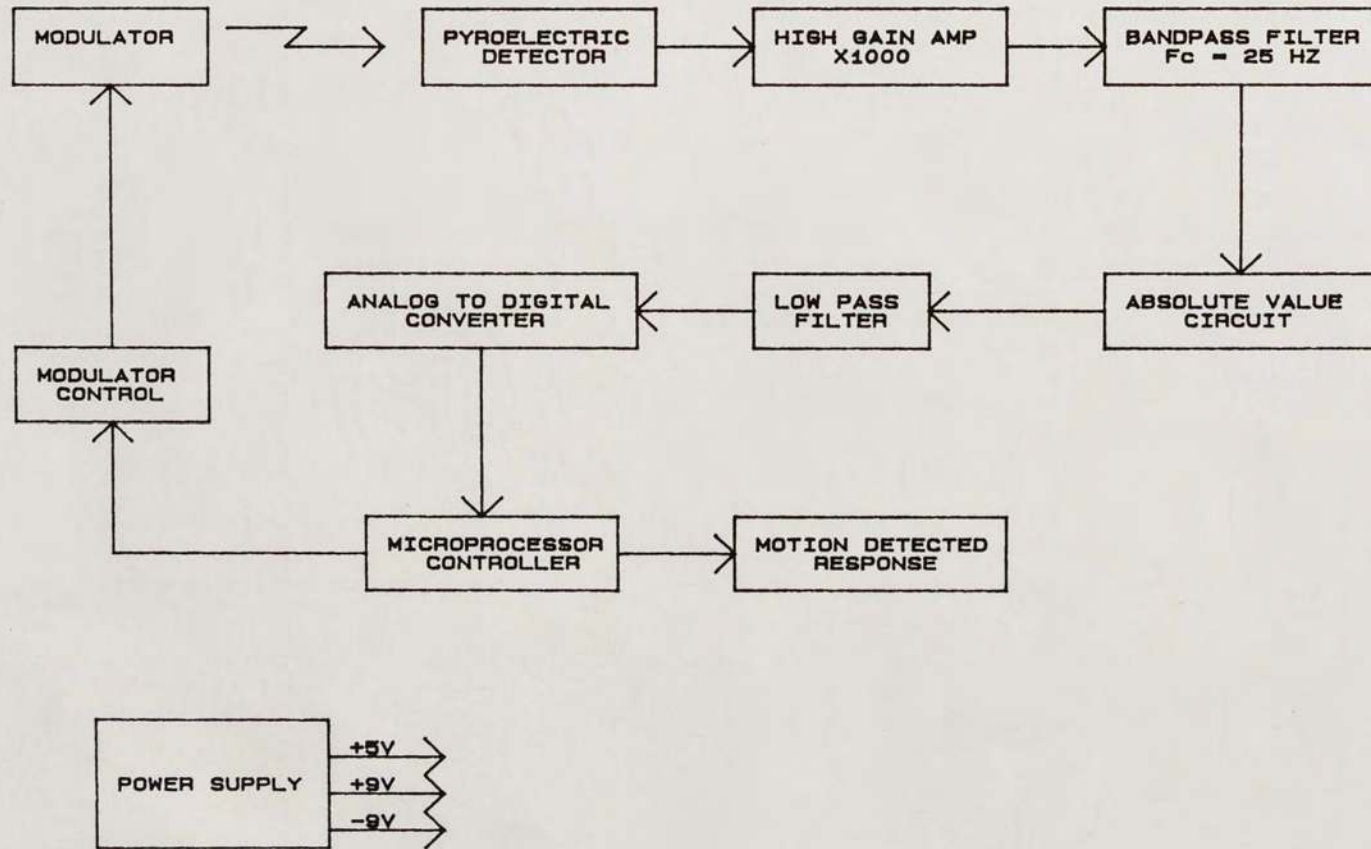


Figure 5. Device Block Diagram

phototransistor to conduct when it passes in front of the LED. The time between each pulse generated by the circuitry of the phototransistor for every revolution of the small disk is measured by the microprocessor. When the time between pulses is too short or too long the duty cycle of the PWM pulse stream is changed to vary the motor supply voltage, thereby completing the control loop and providing the necessary control of the modulation frequency.

## AMPLIFICATION

The response of the detector must be amplified to produce a signal that can be processed by the controller. The output of the detector is a high impedance signal and must not be heavily loaded. A field effect transistor input amplifier was designed in the first source-second collector configuration. The field effect transistor will provide the amplifier with a very high input impedance (on the order of  $10^7$  ohms) to minimize degradation of the input signal.

The amplifier configuration used for the detector response is shown in Figure 7.

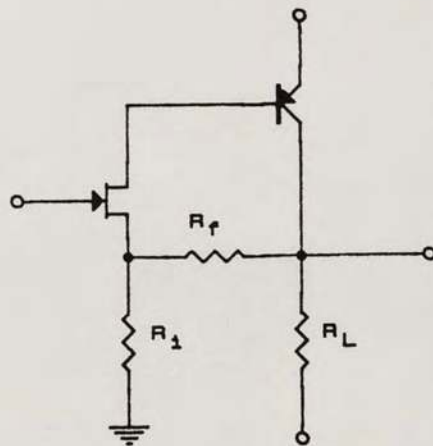


Figure 7. First-Source Second-Collector Configuration

The approximate AC equivalent models for bipolar and field effect transistors are shown in Figure 8.

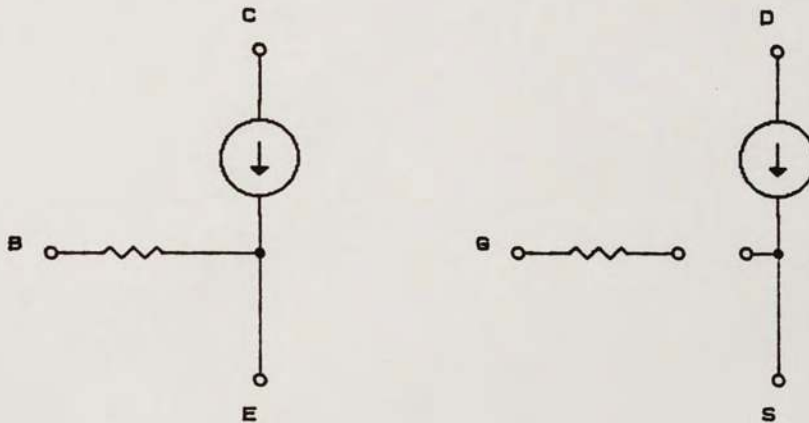


Figure 8. AC Models for Bipolar and Field Effect Transistors

Substituting these models into the circuit as shown in Figure 9 provides an analysis model for the amplifier. The resistor that was part of the bipolar model is in series with a current source and will not have an effect on the analysis of the circuit. After eliminating this part the circuit model can be drawn as shown in Figure 10.

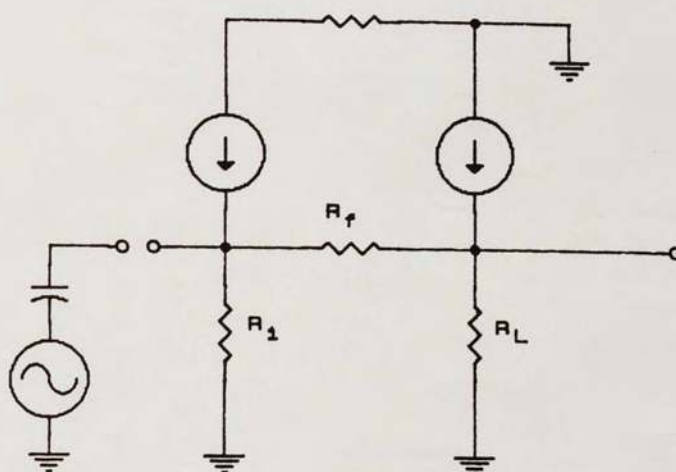


Figure 9. Analysis Model for the Amplifier

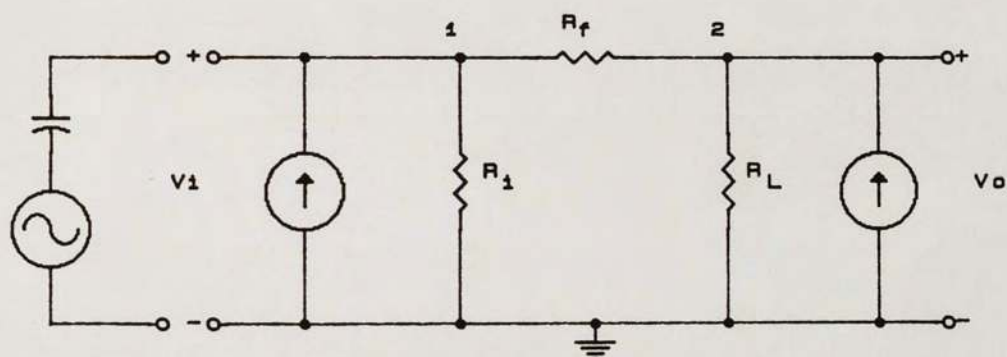


Figure 10. Simplified Analysis Model

Using Kirchoff's current law, equations can be written for nodes 1 and 2 as follows:

$$\frac{V_L + V_O}{R_f} + \frac{V_L}{R_L} - g_{fs}V_{gs} = 0$$

$$\frac{V_O - V_L}{R_f} + \frac{V_O}{R_L} - \beta g_{fs} V_{gs} = 0$$

The first equation can be expressed as:

$$\frac{V_L}{R_f} + \frac{V_L}{R_L} - \frac{V_O}{R_f} = g_{fs} V_{gs}$$

or

$$V_L \left[ \frac{1}{R_f} + \frac{1}{R_L} \right] - V_O \frac{1}{R_f} = g_{fs} V_{gs}$$

Repeating for the second equation yields:

$$- \frac{V_L}{R_f} + \frac{V_O}{R_f} + \frac{V_O}{R_L} = \beta g_{fs} V_{gs}$$

or

$$- V_L \left[ \frac{1}{\beta R_f} \right] + V_O \left[ \frac{1}{\beta R_f} + \frac{1}{\beta R_L} \right] = g_{fs} V_{gs}$$

Now combining the two equations yields

$$V_L \left[ \frac{1}{R_f} + \frac{1}{R_i} \right] - V_O \left[ \frac{1}{R_f} \right] = -V_L \left[ \frac{1}{\beta R_f} \right] + V_O \left[ \frac{1}{\beta R_f} + \frac{1}{\beta R_L} \right]$$

$$V_L \left[ \frac{1}{R_f} + \frac{1}{R_i} + \frac{1}{\beta R_f} \right] = V_O \left[ \frac{1}{\beta R_f} + \frac{1}{\beta R_f} + \frac{1}{R_L} \right]$$

Now:

$$V_L \left[ \frac{\beta R_i + \beta R_f + R_i}{\beta R_f R_i} \right] = V_O \left[ \frac{R_L + R_f + \beta R_L}{\beta R_f R_L} \right]$$

$$\frac{V_O}{V_i} = \left[ \frac{\beta R_i + \beta R_f + R_i}{R_i} \right] \left[ \frac{R_L}{R_L + R_f + \beta R_L} \right]$$

$$= \left[ \beta \left\{ 1 + \frac{R_f}{R_i} \right\} + 1 \right] \left[ \frac{1}{\frac{R_L + R_f}{R_L} + \beta} \right]$$

Since

$$\beta \left\{ 1 + \frac{R_f}{R_i} \right\} \gg 1 \quad \text{and} \quad \frac{R_L + R_f}{R_L} \ll 1$$

the expression becomes

$$\frac{V_O}{V_i} \approx \frac{1 + \frac{R_f}{R_i}}{1 + \frac{R_L + R_f}{R_L}} \approx \left[ 1 + \frac{R_f}{R_i} \right]$$

The input resistance of the circuit would be very high as can be seen from the model of the amplifier.



## BAND PASS FILTER DESIGN

Placed between the high gain amplifier and the absolute value circuit is a band pass filter. The center frequency of the pass band is 25 Hz. The modulation frequency of the incoming IR energy is controlled by the microprocessor to be between 24 and 26 Hz. These frequencies were selected to be the corner frequencies of the pass band. Another criterion for the filter was to minimize the effect of signals generated by the 60Hz, 120V commercial power lines. The pass band should therefore attenuate signals at this frequency heavily. The desired frequency response of the filter is as shown in Figure 11.

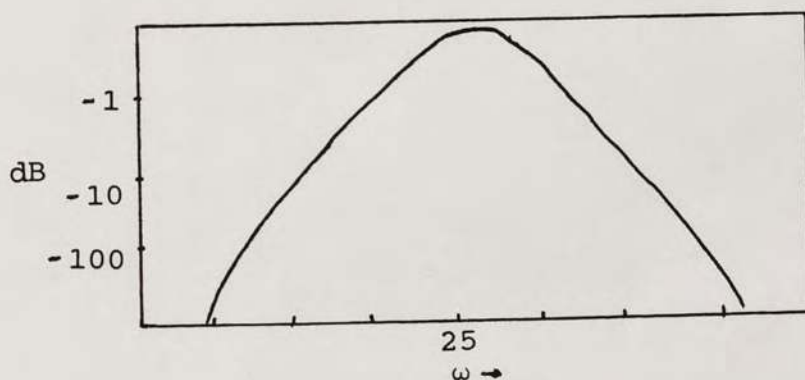


Figure 11. Frequency Response of the Filter

The Q of the circuit will be

$$Q = \frac{F_c}{F_h - F_l} = \frac{25}{26 - 24} = 12.5$$

The band pass filter configuration selected has second order transfer function and is schematically shown in Figure 12.

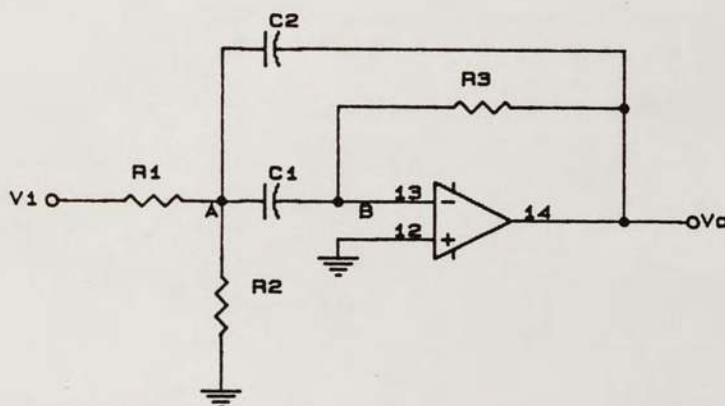


Figure 12. Schematic of the Filter

The analysis of this circuit is as follows:

Node equation for Node A:

$$\frac{V_a - V_i}{R_1} + \frac{V_a}{R_2} + [V_a + V_b] C_1 s + [V_a - V_o] C_2 s = 0$$

$$V_a \left[ \frac{1}{R_1} + \frac{1}{R_2} + C_2 s + C_1 s \right] - V_b C_2 s - \frac{V_i}{R_1} - V_o C_1 s = 0$$

Node equation for Node B:

$$[V_b - V_a] C_2 s + \frac{V_b}{R_4} + \frac{V_b - V_o}{R_3} = 0$$

$$V_b \left[ C_2 s - \frac{1}{R_4} + \frac{1}{R_3} \right] = V_a C_2 s + V_o \frac{1}{R_3}$$

But  $V_b = 0$

$$V_a C_2 s + \frac{V_o}{R_3} = 0 \quad \text{or} \quad V_a = - \frac{V_o}{R_3 C_2 s}$$

Now substituting  $V_a$  back into the first equation yields:

$$\frac{V_o}{R_3 C_2 s} \cdot \frac{R_1 + R_2 + R_1 R_2 (C_1 + C_2) s}{R_1 R_2} = \frac{V_i}{R_1} + V_o C_1 s$$

$$\frac{V_i}{R_1} = - V_o \left[ \frac{R_1 + R_2 + R_1 R_2 (C_1 + C_2) s}{R_1 R_2 R_3 C_2 s} \right] + C_1 s$$

or

$$\frac{V_o}{V_i} = - \frac{R_2 R_3 C_2 s}{R_1 + R_2 + R_1 R_2 (C_1 + C_2) s + R_1 R_2 R_3 C_1 C_2 s^2}$$

A general transfer function that provides the band pass characteristic is

$$\left| H(s) \right| = \frac{A_0 \frac{s}{\omega_c Q_c}}{\frac{s^2}{\omega_c^2} + \frac{1}{\omega_c Q_c} + 1}$$

Rearranging the expression for  $V_o/V_{in}$  above yields

$$\frac{V_o}{V_i} = - \frac{R_2 R_3 C_2 s}{R_1 R_2 R_3 C_1 C_2 s^2 + R_1 R_2 (C_1 + C_2) s + R_2 + R_1}$$

Equating like terms yields

$$\frac{1}{\omega_c^2} = \frac{R_1 R_2 R_3 C_1 C_2}{R_1 + R_2}$$

$$\omega = \left[ \frac{R_1 + R_2}{R_1 R_2 R_3 C_1 C_2} \right]^{1/2}$$

From the coefficient for the  $s$  terms

$$\frac{1}{\omega_c Q_c} = \frac{R_1 R_2 (C_1 + C_2)}{R_1 + R_2}$$

and

$$\frac{A_0}{\omega_c Q_c} = \frac{R_2 R_3 C_2}{R_1 + R_2}$$

Now

$$\frac{R_1 R_2 (C_1 + C_2)}{R_1 + R_2} = \frac{R_2 R_3 C_2}{A_0 (R_1 + R_2)}$$

and

$$A_0 = \frac{R_3 C_2}{R_1 (C_1 + C_2)}$$

Substituting the previously determined value for  $c$  into

$$\frac{1}{\omega Q_C} = \frac{R_1 R_2 (C_1 + C_2)}{R_1 + R_2}$$

yields

$$\frac{1}{Q_C} = \frac{R_1 R_2 (C_1 + C_2)}{R_1 + R_2} \cdot \left[ \frac{R_1 + R_2}{R_1 R_2 R_3 C_1 C_2} \right]^{1/2}$$

or

$$Q_C = \frac{1}{C_1 + C_2} \cdot \left[ \frac{(R_1 + R_2) R_3 C_1 C_2}{R_1 R_2} \right]^{1/2}$$

Selecting values for the components:

Let  $C_1 = C_2 = C$ ; the equations would become

$$\omega_c = \left[ \frac{R_1 + R_2}{R_1 R_2 R_3} \right]^{1/2} \frac{1}{C}$$

$$A_o = \frac{R_3}{2R_1}$$

$$Q_c = \left[ \frac{(R_1 + R_2)R_3}{4R_1 R_2} \right]^{1/2}$$

Starting with  $A_o = 1$ :

$$A_o = 1 = \frac{R_3}{2R_1}$$

$$Q_c = \frac{(R_1 + R_2)2R_1}{4R_1 R_2} \left[ \frac{R_1 + R_2}{2R_2} \right]^{1/2} \frac{1}{C}$$

Let  $C = 1.0\mu\text{F}$ .

Then

$$R_1 (1.0 \times 10^{-6}) = \frac{12.5}{2\pi (25)}$$

$$R_1 = 79.577 \times 10^3 \text{ ohms}$$

The closest 1% resistor value would be  $80.6\text{K}\Omega$  .

$R_3$  now becomes:

$$R_3 = 2R_1 = 2(80.6 \times 10^3) = 161.2 \text{ Kohms}$$

The closest 1% value for  $R_3$  would be 162K $\Omega$ .

Now solving for  $Q_C$ :

$$Q_C = \left[ \frac{R_1 + R_2}{2R_2} \right]^{1/2}$$

$$2R_2Q_C^2 = R_1 + R_2$$

$$R_2(2Q_C^2 - 1) = R_1$$

$$R_2 = \frac{R_1}{(2Q_C^2 - 1)} = \frac{80.6 \times 10^3}{2(12.5)^2 - 1} = 258 \text{ ohms}$$

The closest 1% component value for  $R_2$  would be 255 ohms.

## ABSOLUTE VALUE CIRCUIT

The absolute value circuit rectifies the input signal for negative swings.

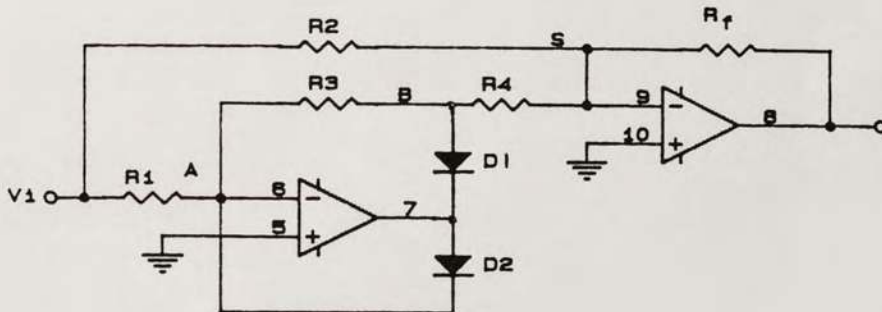


Figure 13. Absolute Value Circuit

The circuit can be treated for negative and positive inputs separately[5].

For negative input voltages the output of the first amplifier section would be positive, which would reverse bias  $D_1$  and forward bias  $D_2$ . The circuit would behave as though  $D_1$  were not present as shown in Figure 14. The output of the amplifier would be clamped to a voltage very close to ground through  $D_2$ . The first op-amp would have no effect on the input signal and the circuit would effectively behave as shown in Figure 15.



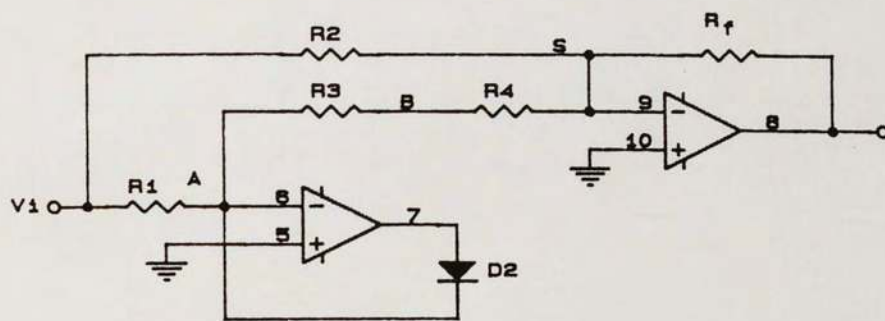


Figure 14. Model for Negative Inputs

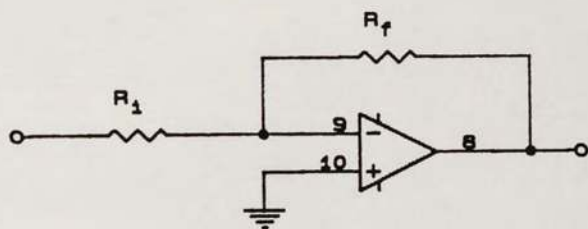


Figure 15. Simplified Circuit for Negative Signals

Where

$$V_o = -\frac{R_f}{R_1} V_i$$

Substituting the values for the resistors yields

$$V_o = -\frac{R}{R} V_i$$

or

$$V_o = -V_i$$

For positive input voltages the output of the first stage would be negative, reverse biasing  $D_2$  and forward biasing  $D_1$ . Again assuming that  $D_1$  acts as a short, the circuit would behave as shown in Figure 16.

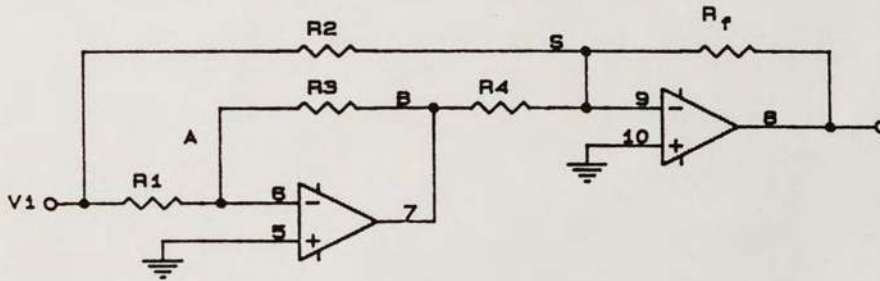


Figure 16. Model for Positive Inputs

An analysis of the circuit would proceed as follows:

Node equations for Node A

$$\frac{V_a - V_i}{R_1} - \frac{V_a - V_b}{R_3} = 0$$

$$V_a \left[ \frac{1}{R_1} + \frac{1}{R_3} \right] - \frac{V_i}{R_3} = \frac{V_b}{R_3}$$

But since  $V_a = 0$ :

$$V_b = - \frac{V_i R_3}{R_1}$$

For node S:

$$\frac{V_S - V_i}{R_2} + \frac{V_S - V_b}{R_4} + \frac{V_S - V_o}{R_f} = 0$$

$$V_S \left[ \frac{1}{R_2} + \frac{1}{R_4} + \frac{1}{R_f} \right] = \frac{V_i}{R_2} + \frac{V_b}{R_4} + \frac{V_o}{R_f}$$

Now substituting the previously derived value of  $V_b$  and noting that  $V_S = 0$  gives:

$$\frac{V_i}{R_2} + \frac{V_i R_3}{R_1 R_4} + \frac{V_o}{R_f} = 0$$

$$\frac{V_o}{R_f} = V_i \left[ \frac{1}{R_2} - \frac{R_3}{R_1 R_4} \right]$$

$$\frac{V_o}{V_i} = \frac{R_f R_1 R_4 - R_2 R_3 R_f}{R_1 R_2 R_4}$$

Substituting in the values of the resistors yields

$$\frac{V_o}{V_i} = \frac{4R^3 - 2R^3}{2R^3} = 1$$

or

$$V_o = V_i$$

Summarizing,

$$V_o = \begin{cases} V_i & \text{for } V_i > 0 \\ -V_i & \text{for } V_i < 0 \end{cases}$$

The transfer characteristic is as shown in Figure 17.

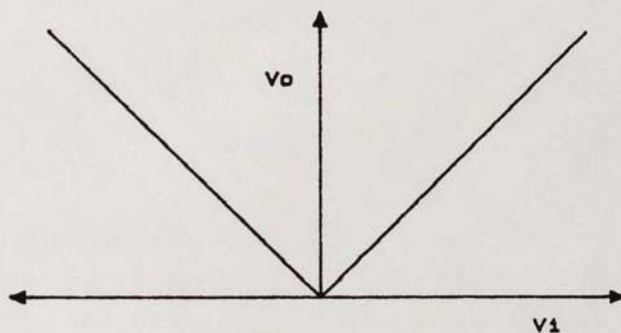


Figure 17. Transfer Characteristic of the Absolute Value Circuit

## SIGNAL PROCESSING

To convert the analog signal output of the absolute value circuit to a digitally processable signal, a low-pass filter followed by an analog-to-digital converter is used. The NE5037 is a 6-bit successive approximation type analog to digital converter (ADC). The reference voltage for the ADC is 3V which provides a 0.047 volt/bit resolution to the microprocessor. When a conversion needs to be performed the microprocessor asserts the START pin on the ADC and polls the CONVERSION COMPLETE pin to determine when the converted data is ready to be read.

The microprocessor used in this system is an Intel 8049 microcontroller. This controller has 16 I/O ports available along with two test inputs to provide an interface to the external circuit. The clock frequency of the processor is 6 Mhz, which gives the internal timer function an 80 uS clock period. The internal timer is used to monitor real time events such as the modulator motor speed control.

## SUMMARY

A method of passively detecting the presence of a warm object in a designated area has been presented. The system is based on a detector that utilizes the pyroelectric effect to convert the heat generated by the object into a voltage signal that can be processed and used to indicate the presence of the object. The heat generated in the form of infrared energy was focused onto the detector which resulted in a slight temperature change of the pyroelectric crystal. The change in temperature caused a change in the natural spontaneous polarization of the crystal and a change in the surface charge present. The change in surface charge caused a transient potential difference across the electrodes of the detector. This response was amplified and sampled by a microprocessor to indicate the presence of the object.

The device could be used in the area of intruder detection for security systems. Another application of the device would be in a manufacturing environment to count the number of warm objects passing by on an assembly line. With appropriate optical filtering the device could also be used for fire detection.

APPENDIX

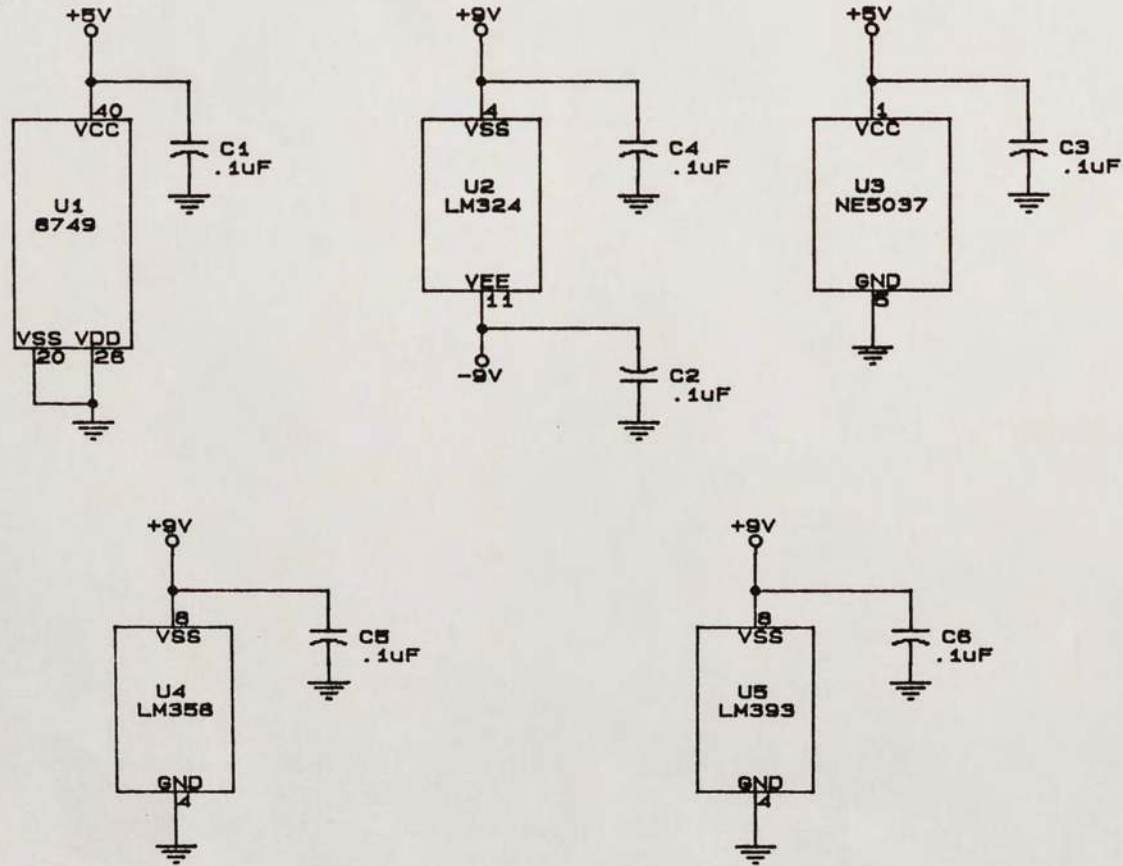


Figure 18. Power and Ground Connections



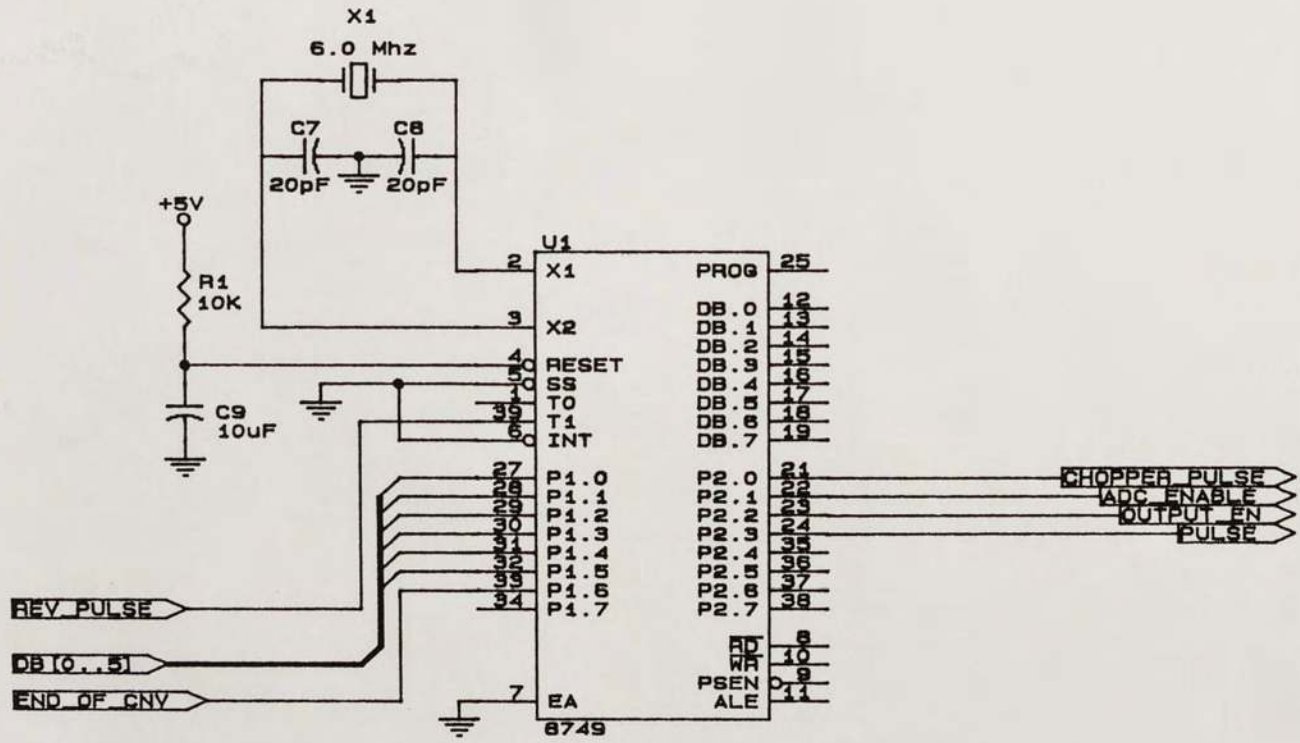


Figure 19. Microcontroller

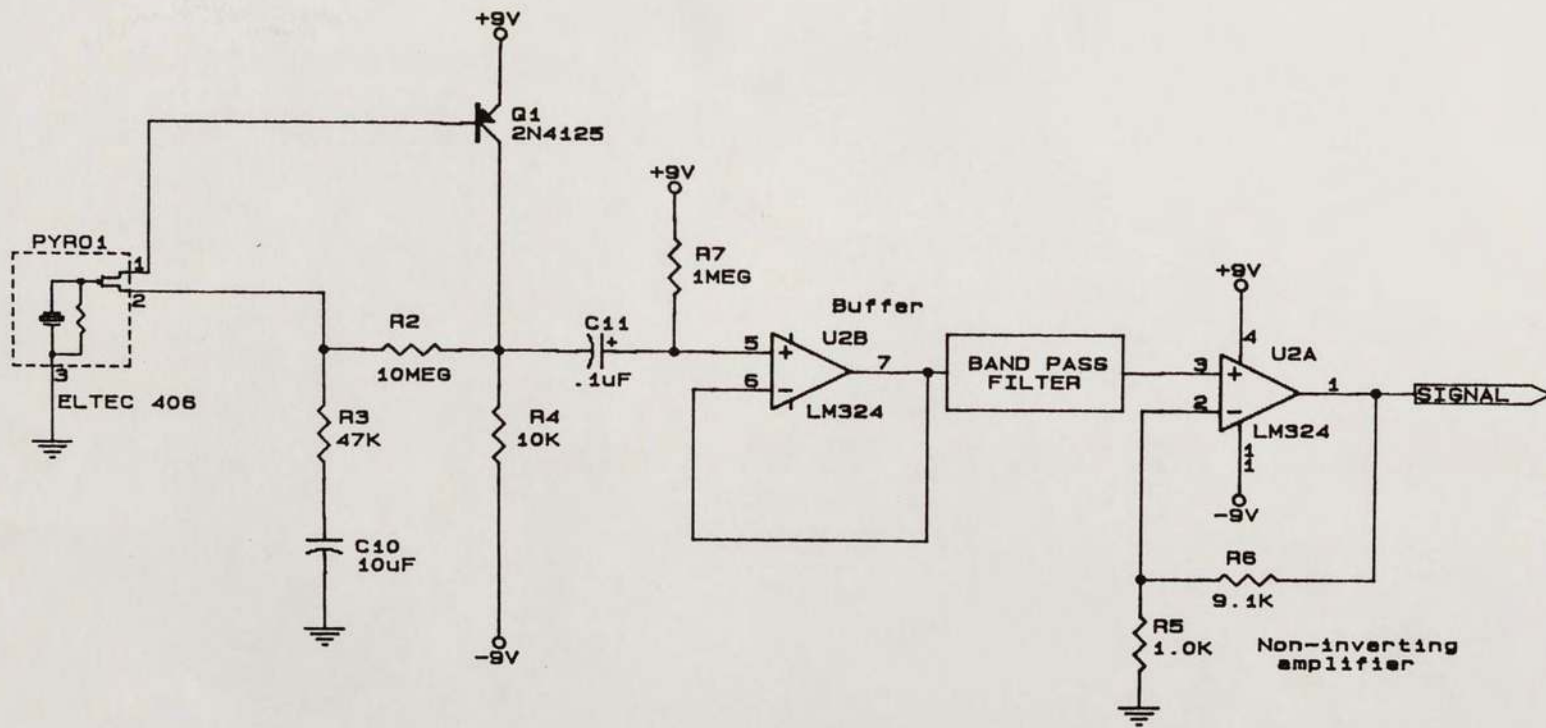


Figure 20. Detector Amplifier

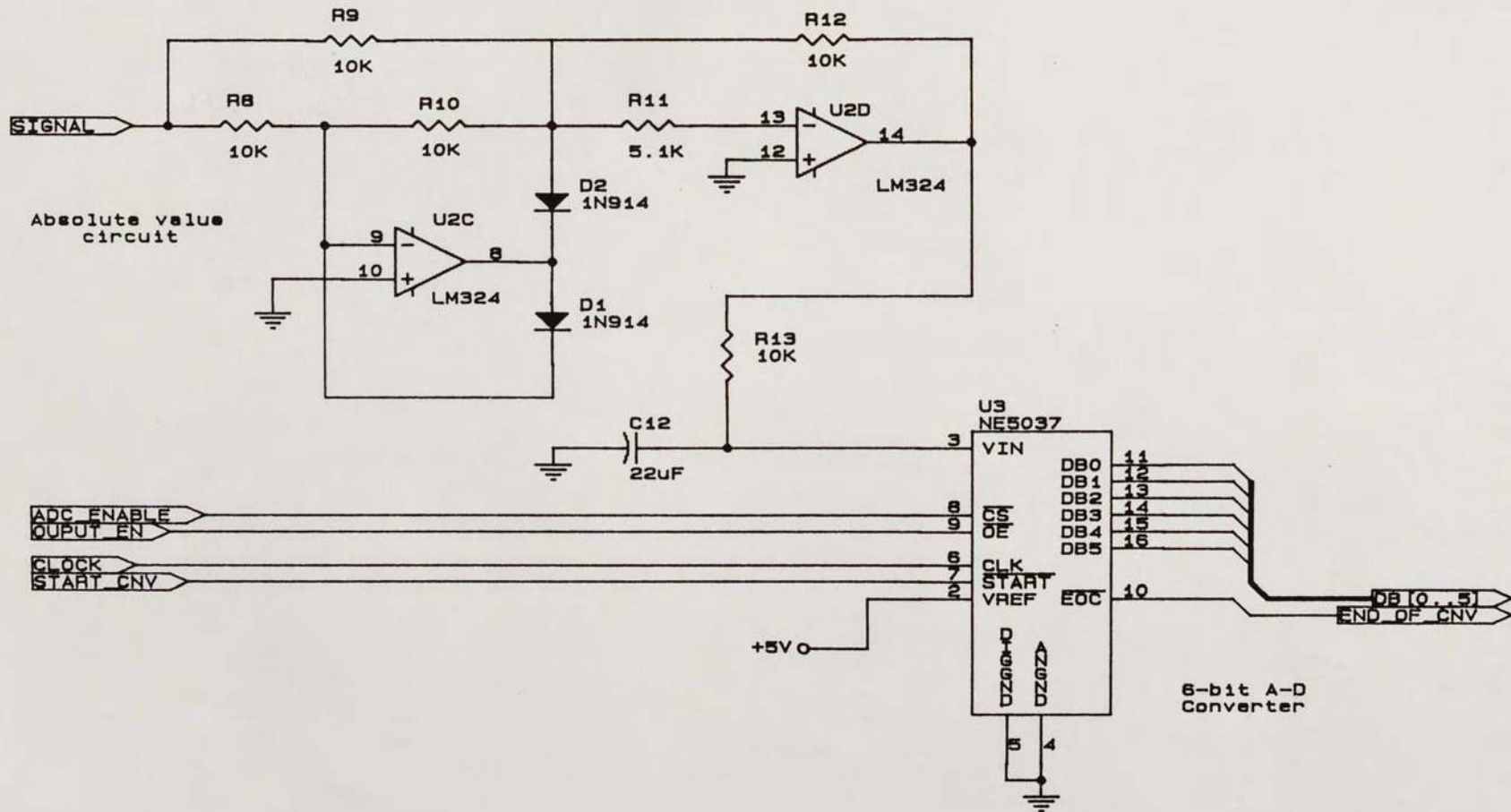


Figure 21. Signal Processor

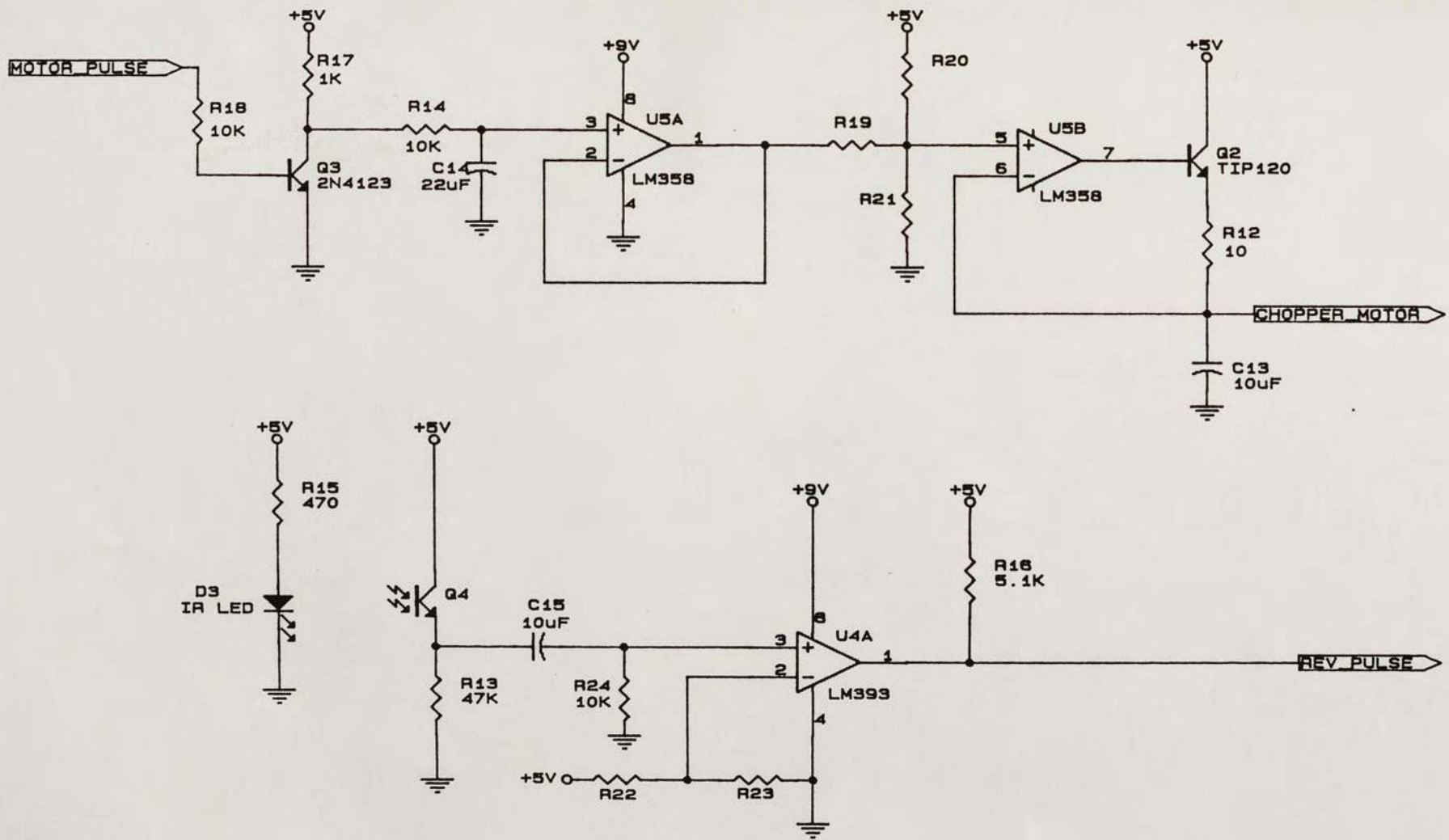


Figure 22. Motor Control Circuitry

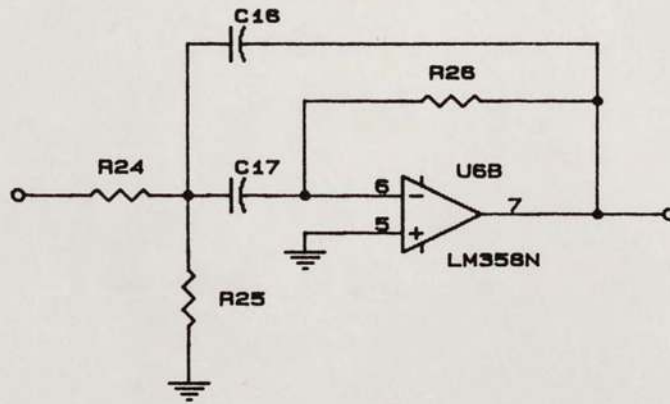


Figure 23. Band Pass Filter

## SOFTWARE LISTING FOR MOD.001

```
; This code keeps a constant 1Khz pulse train of
; variable pulse width going for the chopper motor. The
; period of rotation of the chopper is monitored and the
; duty cycle of the pulse train is changed to vary the
; voltage supplied to the motor. An analog-to-digital
; conversion is also performed every .1 seconds on the
; detector output. When the threshold value is detected
; the buzzer is turned on. Otherwise the buzzer is
; turned off.
```

```
CLK_PER EQU      0F3H          ; Clock period = 1ms

      ORG        0
      JMP        START

      ORG        7
TIMER: SEL        RB1
      MOV        R6, A          ; R6 is loc 30
      MOV        A, #CLK_PER
      MOV        T, A
      MOV        A, R4          ; R4 is current pw
      MOV        R3, A
      ORL        P2, #00010000B ; Pulse line high
TLOOP: DJNZ       R3, TLOOP     ; R3 = amount of time
                                      ; pulse line is low

      CLR        A
      ANL        P2, #11101111B ; Pulse line low
      JNT1       NEW           ; Look for trailing edge
      JF0        RND           ; Flag = 0 says already
                                      ; adjusted for pulse

      CLR        F0
      CPL        F0
      MOV        A, R5
      ADD        A, #173        ; 256 - 173 = 83
      JNC        TOOFST
      JF1        TLA           ; Settle time for new
                                      ; pulse width

      CPL        F1
      DEC        R4
TLA:  CLR        A
      MOV        R5, A
      JMP        RND
```

```

TOOFST: MOV     A, R5
        ADD     A, #187           ; 256 - 187 = 69
        JC      TFL
        JF1     TFL
        CPL     F1
        INC     R4
TFL:    CLR     A
        MOV     R5, A
        JMP     RND
NEW:    CLR     F0
RND:    INC     R5
        INC     R7               ; R7 is the system
                                   ; clock, LOC 31
        MOV     A, R6
        SEL     RB0
        RETR

START:  MOV     A, #CLK_PER       ; Start system timer
        MOV     T, A
        EN     TCNTI
        SEL     RB1
        MOV     R4, #20
        CLR     A
        CPL     A
        OUTL    P1, A           ; Initialize ports
        OUTL    P2, A           ; and memory
        MOV     R5, A
        MOV     R7, A
        SEL     RB0
        MOV     R0, #29
        MOV     R1, #31
        MOV     R4, #10
DELB:   MOV     R3, #0FFH
DELA:   MOV     R2, #0
DEL:    DJNZ    R2, DEL         ; Allow transients to
                                   ; settle
        DJNZ    R3, DELA
        DJNZ    R4, DELB
        STRT    T

LOOP:   MOV     A, @R1          ; Main loop begins by
                                   ; Looking for 1/10
                                   ; second mark
        XRL     A, #100
        JZ      LOOPA          ; If found go to loopa
        JMP     LOOP
LOOPA:  CLR     F1             ; Initialize flag
        CLR     A
        MOV     @R1, A

```

```

                CALL    ADIN          ; Perform AD conversion
                JMP     LOOP          ; End of main loop

ADIN:          ANL     P2, #11011111B ; AD handler begins
                NOP
                ORL     P2, #00100000B ; by do a CS on NE5037
                NOP

GTSTAT:       IN      A, P1          ; Look at bit 6 for
                JB6    GTSTAT        ; 'CONVERSION COMPLETE'
                ANL     P2, #10111111B
                NOP
                IN      A, P1
                ORL     P2, #01000000B
                ANL     A, #3FH       ; Clear upper two bits
                ADD     A, #208       ; Look for value
                                        ; greater than 208
                                        ; 256 - 48 = 208
                JC      SOUND        ; If greater than
                                        ; threshold (208) then
                                        ; turn on buzzer
                                        ; Else turn off buzzer

NOSND:        ORL     P2, #80H
                RET

SOUND:        ANL     P2, #7FH       ; Turn on buzzer
                RET

                END

```



## REFERENCES

- [1] S. T. Liu, Donald Long, "Pyroelectric Detectors and Materials", Proceedings of the IEEE 66 (January 1978): 14.
- [2] E. Fatuzzo, W. J. Merz, Ferroelectricity (Amsterdam: North-Holland Publishing Company, 1967), p. 63-76.
- [3] Walter Cady, Piezoelectricity (New York: Dover Publications, Inc. 1964), p. 699.
- [4] M. E. Lines, A. M. Glass, Principles and Applications of Ferroelectrics and Related Materials (Oxford: Oxford University Press, 1977) p. 8-9.
- [5] John V. Wait, Lawrence P. Huelmsan, Granino A. Korn, Introduction to Operational Amplifier Theory and Applications (New York: McGraw-Hill Book Company, 1975) p. 171-174.
- [6] Robert J. Keyes, E. H. Putley, Topics in Applied Physics: Optical and Infrared Detectors (New York: Springer-Verlag Berlin Heidelberg, 1977) p. 90-95.
- [7] Eltec Instruments, Inc., "Introduction to Infrared Pyroelectric Detectors", Eltec Instruments Product Catalog (1984) p. 24.